Original Article

ENERGY EXPLORATION & EXPLOITATION

Energy Exploration & Exploitation
2017, Vol. 35(3) 295–314

DOI: 10.1177/0144598717690089
journals.sagepub.com/home/eea
SAGE

Geochemical analysis and origin of gas in volcanic reservoirs in the Songliao Basin

Shizhen Tao,[1] Changwei Li,[1] Weijiao Ma,[1] Deliang Liu,[2] Jingkui Mi[1] and Zhenglian Pang[1]

Abstract

Volcanic reservoirs are extensive in the Songliao Basin and mainly include intermediate-basic rocks in the northern part, intermediate-acidic rocks in Xujiaweizi in the southern part, and acidic rocks in the Jinglin block. The natural gas in the volcanic reservoirs of the Songliao Basin has a wide range of compositions, with alkanes being dominant in most cases, although carbon dioxide is dominant in some wells. Generally, the gas in the volcanic rocks near deep faults has high contents of carbon dioxide, whereas the natural gas in volcanic rocks far from faults has low carbon dioxide contents. The gas in the volcanic reservoirs is of multiple origins, including abiogenic gas of probable mantle origin (generally found in wells with high carbon dioxide contents) and organic gas mainly derived from organic matter in the basin. The abiogenic alkanes have $\delta^{13}C$ values in the order of $\delta^{13}C_1 > \delta^{13}C_2 > \delta^{13}C_3 > \delta^{13}C_4$, which is opposite that of alkanes of organic origin. The $^3He/^4He$ ratios of the fluid inclusions from the volcanic reservoirs range from 0.286×10^{-6} to 7.33×10^{-6}, with an average of 2.48×10^{-6}, and the R/Ra ratios range from 0.26 to 5.24, with most values being greater than 1.0, indicating mixed origins of noble gases from the crust and the mantle. The gas in fluid inclusions from the volcanic reservoirs has $\delta^{13}C_1$ values ranging from −17.1 to −28.7‰ (PDB), $\delta^{13}C_2$ values ranging from −23.4 to −32.4‰ (mostly approximately −25‰), and $\delta^{13}C_{CO_2}$ values ranging from −10.97 to −21.73‰, which are significantly different from the isotopic compositions of the gas in the present reservoirs, suggesting that some abiogenic alkanes may have been charged into the reservoirs during the geologic history of the basin. The early charged CO_2 is mainly organic in origin, while the abiogenic CO_2 was charged during the main accumulation period, producing a mix of origins for the gas in the volcanic reservoirs of the Songliao Basin. The abiogenic alkanes, He, and CO_2 in the natural gas indicate the addition of some abiogenic gas to the gas. According to the relationship between the distribution and attitude of volcanic rocks and faults, we found that the abiogenic gas reservoirs

[1]Research Institute of Petroleum Exploration & Development, PetroChina, Beijing, China
[2]Department of Earth and Space Science, University of Science and Technology of China, Hefei, China

Corresponding author:
Shizhen Tao, Research Institute of Petroleum Exploration & Development, PetroChina, Beijing 100083, China.
Email: tsz@petrochina.com.cn

are located near fault zones, whereas the organic and mixed gas reservoirs are located far from fault zones. The geochemical study of natural gas is helpful in determining the origin and spatial distribution patterns of gas in deep volcanic reservoirs and for directing further gas exploration in the Songliao Basin.

Keywords
Volcanic reservoirs, abiogenic gas, coal-derived gas, carbon isotopes, rare gas isotopes, fluid inclusions, Songliao Basin

Introduction

Gas exploration in volcanic reservoirs faces three problems – gas origin, reservoir control factors, and targets – due to their special composition, environment, and reservoir conditions. The study of gas origin depends on geochemical analysis of gas isotopes (Dai et al., 2005). There are two different viewpoints for the gas formation and distribution in the Songliao Basin volcanic reservoirs: an organic origin, in which the gas is controlled by the lower Cretaceous source rocks; and an abiogenic origin, in which the gas is controlled by magma activity and a deep gas source (Dai et al., 2014). The differences between this paper and previous research lie in the methods. By using the carbon isotopes of carbon dioxide and alkane gas in fluid inclusions from the gas reservoir, the isotopes of He and Ar, and the homogenization temperatures of fluid inclusions, we explain the origin, source, and filling periods of natural gas in the volcanic reservoir in the Songliao Basin.

There are multiple views regarding the causes of the formation of alkane gas in volcanic reservoirs in the Songliao Basin (Dai et al., 2014). (1) Highly overmatured coal-derived gas. The heavy carbon isotope values of methane and the carbon isotope antitone, or negative carbon isotope series, i.e. $\delta^{13}C_1 > \delta^{13}C_2 > \delta^{13}C_3 > \delta^{13}C_4$, in natural gas in the deep layer of the northern Songliao Basin are due to highly overmatured coal measure source rocks (Huang, 1996; Ren et al., 2004; Yang et al., 2002). The Kela-2 gas field and the Dabei gas field in the Tarim Basin were formed in highly overmatured middle–upper Jurassic coal measures. Although there are isotopic reversals in the two fields, they basically exhibit a positive sequence. Negative carbon isotope series do not appear in the alkane gas formed in highly overmatured coal measures in the Central Europe Basin. For example, in Germany's Northwest Basin, highly overmatured Carboniferous coal measures generated the gas. The $\delta^{13}C_1$, $\delta^{13}C_2$, and $\delta^{13}C_3$ values of the gas from well T_1 in the Mickelson gas field are −26.6, −23.7, and −23.1‰, respectively, and the $\delta^{13}C_1$, $\delta^{13}C_2$, and $\delta^{13}C_3$ values of the gas from well Z_1 are −28.9, −23.0, and −21.0‰, respectively (Dai et al., 2014). (2) Deep organic source gas. The gas with abnormal geochemical characteristics from the deep Songliao Basin is called deep organic source gas and was speculated to be derived from the deeply buried slate and phyllite (Gao and Cai, 1997). (3) Mix of different types of natural gas and micro-leakage of cap rocks. The gas in the deep part of the Songliao Basin is thought to be organic in origin, but the gas isotopic reversal is caused by fractionation effects due to the mixing of different types of gas and micro-leakage through the cap rock (Huang, 2000). (4) Mix of coal-derived gas and a small amount of inorganic alkane gas (Feng, 2008; Li et al., 2009). (5) Inorganic gas and a small amount of coal-derived gas (Dai et al., 2005; Guo and Wang, 1994; Wang et al., 2006). The last two hypotheses have the most support. The origin of the alkane gas, i.e. oil derived or coal derived, in the Songliao Basin is discussed in the following study based on the latest data.

This paper analyses the source, origin, and distribution features of the CO_2-rich gas in volcanic reservoirs in the Songliao Basin; presents the geologic distribution of volcanic reservoirs based on gas geochemistry, isotope geochemistry, and fluid inclusion methods; and proposes further exploration approaches and directions.

Regional geologic setting

The Songliao Basin is located in the northeast of China (Figure 1) and represents an intracontinental rift basin. The depression contains four sets of source rocks: Huoshiling, Shahejie, Yingcheng, and Denglouku Formations from the bottom to the top. The Shahejie Formation is the main source rock and is capable of generating coal-derived gas (Dai et al., 2014). The TOC of this formation is 0.53–14.63%; the organic material is mainly type II_2 and III; the Ro is above 2.0%; and the hydrocarbon potential is 0.52–4.08 mg/g. During the rifting period in the Cretaceous and early Jurassic, deep faults, volcanic conduits, and volcanic rocks developed, which enabled the formation of inorganic mantle-released gas. Thus, the rifting period was favourable for both coal series gas and mantle released gas.

The Songliao Basin comprises strata from the Carboniferous to the Cretaceous Quantou Formation. During the Yanshanian period, the subduction of the Pacific plate beneath the Eurasian plate caused intracontinental rifting in the Songliao area and considerable volcanic activity. The explosive and effusive facies are favourable reservoir rocks for natural gas. The volcanic reservoirs are fairly good in terms of physical properties but feature obvious

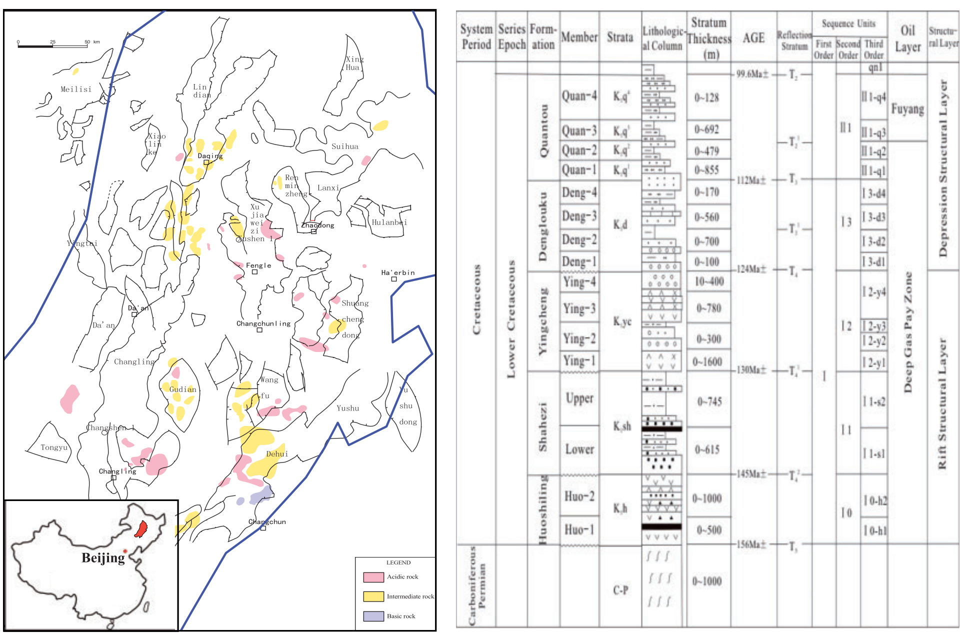

Figure 1. Volcanic rock distribution and composite stratigraphic column of the Songliao Basin (Dai et al., 2014).

heterogeneity, with porosity values of 0.5–18.7% and permeability values of 0.0001×10^{-3}–$1 \times 10^{-3}\,\mu m^2$ (Feng, 2008). At present, two giant gas fields have been discovered in the northern Xujiaweizi and southern Changling rifts in the Songliao Basin (Figure 1).

The strata in the basin are divided into deep strata and the middle-shallow strata (Figure 1). The deep strata of the Songliao Basin refer to the rocks underlying the Quan-2 member of the Cretaceous Quantou Formation (Figure 1), and the volcanic gas prospecting targets include Huoshiling, Shahezi, and Yingcheng Formations at depths of 3000–5000 m. The rifting sequence is composed of three sets of volcanic rocks and four sets of clastic rocks (Figure 1). The Ying-4 member of the Yingcheng Formation in the Cretaceous system is dominated by conglomerate, sand, and mudstone in the lower part; the Ying-3 member is characterized by interbedded intermediate-basic volcanic rocks and acidic volcanic rocks; the Ying-2 member mainly consists of clastic rocks; and the Ying-1 member is a set of acidic volcanic rocks. The Shahezi Formation is a set of coal-bearing clastic rocks. The Huo-2 member contains intermediate-basic volcanic rocks, and the Huo-1 member includes coal-intercalated clastic rocks. The gas-bearing zones are mainly present in the Yingcheng volcanic rocks, followed by the clastic rocks in the Yingcheng, Shahezi, and Denglouku Formations.

Studies show that basic and acidic volcanic rocks coexist in the Daqing blocks of the Songliao Basin. In addition to large amounts of effusive lava, pyroclastic rocks and fallout facies sedimentary volcanic rocks, there are secondary volcanic facies, such as diabase, basaltic trachyte, rhyolite, porphyrite, and intermediate-acidic intrusive rocks. The northern part of the basin mainly consists of intermediate-basic rocks, Xujiaweizi in the south part of the basin is dominated by intermediate-acidic rocks, and the Jinglin block is dominated by acidic rocks.

Photomicrographs of 84 thin sections show there are four volcanic rock facies in the Songliao Basin (Table 1): (1) subvolcanic facies: mainly diabase, basaltic trachyte, andesite, and rhyolite porphyrites; (2) effusive facies: trachyte, trachydacite, basaltic andesite, andesite, dacite, and rhyolite; (3) explosive facies: mainly pyroclastic breccia, tuff, tuffaceous ignimbrite; and (4) sedimentary volcanic facies: sedimentary breccia and tuff dominated by pyroclastic deposits and tuffaceous conglomerate and sandstone.

Samples and analytical methods

One hundred samples of volcanic rocks and clastic rocks (approximately 75% are volcanic rocks) from the natural gas reservoirs were collected from the Xujiaweizi fault depression and its vicinity in the northern Songliao Basin and from the Changling fault depression and its vicinity in the southern Songliao Basin. The samples are used for analyses of fluid inclusions, alkane gas, carbon isotopes of CO_2, He–Ar isotopes, homogenization temperatures, salinity, and Grain containing oil inclusion.

The experiments were conducted at the Central Laboratory of Geosciences and Langfang Branch, Research Institute of Petroleum Exploration and Development (RIPED), PetroChina. The experiments were based on Chinese National standard SY/T6010-1994 and were performed using a Zeiss Axioskop multifunction microscope and a liquid nitrogen Linkam TMS94 microscope stage. The samples are first crushed before extracting the gas from inclusions, then 10–20 g of treated sample is placed in a vacuum tank with four 10 mm diameter steel alloy balls. The tank is subjected to vacuum for 30–50 min. The evacuated tank is then fixed in a crushing machine for 15–20 min. The gas composition analysis is

Table 1. Lithologies, lithofacies, and origin of the volcanic/clastic rocks in the Songliao Basin.

Number	*Sample number*	*Depth (m)*	*Lithology*	*Lithofacies*
1	Changshen-1	3574.70	Rhyolitic crystal pyroclaste, magmatic tuff	Explosive sediments
2	Changshen-103	3725.80	Tuffy-breccia-bearing carbonate vein	Formation of thermo-fluid
3	Changshen-1-1	3728	Oil-bearing acid volcanic breccia	Explosive sediments or volcano pipe
4	Changshen-1-2	3612	Rhyolitic crystals, magmatic tuff	Explosive sediments
5	Changshen-3	2669.90	Eroded quartz syenitic porphyry	Secondary intrusive rocks (subsidiary volcanoes)
6	Dashen-2	3861.24	Feldspar-fragment greywacke	Sediments in volcanic basin
7	Deshen-5	285.80	Dacite	Explosive sediments
8	Du-13	1934.70	Basaltic porphyry or basalt	Hypabyssal rocks or explosive flowing sediments
9	Fangshen-1	3024.23	Feldspar-fragment sandstone	Sediments in volcanic basin
10	Fangshen-2	2889.83	(Irony) Feldspar-fragment sandstone	Sediments
11	Fangshen-7	3172.9–3189.27	Feldspar-fragment sandstone	Sediments in volcanic basin
12	Gu-7	1550	Feldspar-fragment sandstone	Sediments
13	Gushen-1	4489.92	Trachytic tuffy breccia	Explosive sediments
14	Laoshen-1	3561.90	Eroded dacite porphyry	Explosive flowing sediments, postreformed by thermo-fluid
15	Pushen-1	5344.50	Tectonic-broken basaltic tuff	Tectibuc-broken thermo-fluid-modified explosive sediments
16	Shangshen-2	3249.18	Rock fragment-bearing quartz vein	Thermo-fluid
17	Shengshen-201	3581.60	Oolitic siliceous limestone	Sediments
18	Shengshen-7	3726.8–3735.96	Breccia calcite vein	Tectonic and thermo-fluid formed
19	Songshen-1	3479.42	Tuffy sandstone	Sediments in volcanic basin
20	Songshen-3	3290.54	Amygdaloidal basalt	explosive flowing sediments
21	Tongshen-1	57.2/3	Feldspar-fragment sandstone	Sediments in volcanic basin
22	Tuoshen-1	2434	Arkosite dike intercolated andesite porphyry	Intrusive rock superimposed with thermo-fluid vein
23	Wan-17	1314.36	Feldspar-fragment packsand	Sediments
24	Wang-904	2968.92	Broken rhyolitic porphyry	Lava or subsidiary volcanic rocks
25	Xushen-1	3525.60	Rhyolitic crystal magmatic tuff	Explosive sediments
26	Xushen-1	3634.80	Breccia spherical trachyte	Explosive flowing sediments
27	Xushen-21	3656–3661	Amygdaloidal trachyte	Explosive flowing sediments
28	Xushen-6	3846.62	Amygdaloidal trachyte	explosive flowing sediments
29	Xushen-9	3878.69	Breccia-bearing dacite	Explosive flowing sediments
30	Zhaoshen-1	1.3/5	Feldspar-fragment sandstone	Sediments
31	Zhaoshen-3	288,691–2902.1	Granite	Intrusive rocks

performed on an Agilent6890N gas chromatograph with HC flame and thermal conductivity detectors, and the component content is measured and calculated in mole fraction. The gas carbon isotope ratio determination was performed using a Delta Plus XL gas chromatography combustion isotope ratio mass spectrometer (GC-C-IRMS). The chromatographic analyses involved a 30 m × 0.32 μm PLOT Q column. The temperature is held at 30°C for 5 min, raised to 80°C at a rate of 8°C/min, then raised to 260°C at a rate of 4°C/min. The mass spectrometry conditions include ionization through electron impact with an electron energy of 120 eV and an acceleration voltage of 5 kV. The carbon isotope values are reported in $\delta^{13}C$ relative to the Vienna Pee Dee Belemnite standard.

Helium isotopic measurements were made on a VG5400 mass spectrometer at the Lanzhou Institute of Geology, Chinese Academy of Sciences, China (LIG-CAS). The $^3He/^4He$ ratios are reported relative to the atmospheric ratio (Ra) using the helium value of Lanzhou air as the absolute standard ($Ra = 1.4 \times 10^{-6}$). The reproducibility and accuracy of the $^3He/^4He$ ratios are estimated to be ±3%.

Results and discussion

This section is separated into two parts: results and discussion of the geochemical characteristics and origin of the gas in the volcanic reservoirs of the Songliao Basin.

Results of the experiments and tests

The lithologies and lithofacies of the volcanics, the geochemical parameters of the gas in inclusions, and the gas fields are shown in Tables 1 to 5.

Geochemical composition of volcanic gas

The gas in the volcanic reservoirs of the Songliao Basin varies widely in composition and is mostly alkane gases (Dai et al., 2014), but the gas in some wells is dominated by carbon dioxide (Tables 2 and 3).

Noble gas composition

The isotopic compositions in the rare gas in inclusions from volcanics and sandstones in the northern Songliao Basin are listed in Table 3. The $^3He/^4He$ values of inclusion samples from the volcanic and associated clastic rocks in the northern Songliao Basin are in the range of 0.29×10^{-6}–5.17×10^{-6} (Tao et al., 2012). The R/Ra values (the ratio between the $^3He/^4He$ composition of a sample and the $^3He/^4He$ composition of the air) are relatively high, and most are greater than 0.5.

The carbon isotope analytical results for inclusions in volcanics and associated sandstones in the northern Songliao Basin are listed in Table 4. It can be seen that the $\delta^{13}C_{CH4}$ values vary from –21 to –29‰ and that the $\delta^{13}Cco_2$ values vary from –10 to –19‰ (Table 4). Few differences in the carbon isotope compositions of inclusions exist among the different types of rocks (such as volcanics and sandstones).

Physicochemical parameters of fluid inclusions

The targets for He–Ar isotope analysis are inclusions in calcite and quartz veins in volcanic rocks, calcite fill in pores and vugs of volcanic rocks, and calcite cement in volcanic

Table 2. Gas composition and isotopic composition of certain gas wells in the Songliao Basin (Dai et al., 2014).

			Natural gas components (%)										*Isotopic composition (PDB, ‰)*				
Wells	*Horizon*	*Deep*	CH_4	C_2H_6	C_3H_8	iC_4H_{10}	nC_4H_{10}	iC_5H_{12}	nC_5H_{12}	nC_6H_{14}	N_2	CO_2	$\delta^{13}C_1$	$\delta^{13}C_2$	$\delta^{13}C_3$	$\delta^{13}C_4$	$\delta^{13}C_{CO2}$
B1	K1q3	897.4–1212	77.28	3.690	2.020	0.560	0.660	0.220	0.170	0.12	14.76	0.51	−29.10	−21.26	−19.68	−20.47	
B1	K1q1	1480.0–1487.8	81.74	4.450	1.520	0.330	0.460	0.190	0.140	0.15	9.42	1.58	−27.61	−22.62	−20.56	−20.08	
CS1	K_1yc	3753	74.52	0.65	0.00	0.00	0.00	0.00	0.00	0.00	5.71	19.12	−20.78	−20.73			−5.26
CS1	K_1yc	3594	71.01	1.85	0.11	0.00	0.00	0.00	0.00	0.00	4.19	22.84	−23.00	−26.30	−27.30		−6.8
CS1	K_1yc	3550–3594	66.14	1.52	0.18	0.00	0.01	0.00	0.00	0.00	5.90	26.26	−24.20	−26.90	−27.20	−34.30	
CS1-1	K_1yc	3739	82.32	2.08	0.12	0.00	0.02	0.00	0.00	0.00	4.88	10.58	−22.20	−26.90	−27.00		−7.5
CS1-2	K_1yc	3838	18.56	0.44	0.00	0.00	0.00	0.00	0.00	0.00	3.18	77.81	−25.00				−11.6
CS1-2	K_1yc	3697.0–3704.1	69.86	1.79	0.08	0.00	0.00	0.00	0.00	0.00	5.69	22.59	−14.54	−24.34	−25.44		−6.64
CS103	K_1d	3732.50	61.89	1.57	0.12						4.75	31.67	−22.10	−28.80	−30.90	−33.20	
FS6	K1d2	2755.4–3409.1	81.79	1.19								15.32	−23.60	−29.32			−6.61
FS701	K_1yc	3575–3840	12.43	0.16								86.70	−19.73				−1.82
FS9	K_{1yc}	3602–3620	9.61	0.14								89.73	−27.45	−32.11			−4.06
F1	K1q3	405–421.8	95.78	0.490	0.00	0.010	0.00	0.00	0.00	0.00	2.48	1.23	−48.83	−31.63	−27.63	−28.72	
G9	K1q4	1572.4–1580.2	3.45	0.28	0.03	0.00	0.00	0.00	0.00	0.00	3.63	92.61	−43.97				−8.44
H3	K1yc	1965.4–1978	83.58	7.690	4.150	1.190	1.000	0.390	0.250	0.23	0.92	0.62	−34.55	−25.27	−22.82	−23.13	
N10	K1q3	708–760	93.26	2.760	0.670	0.450	0.00	0.00	0.00	0.00	2.32	0.57	−38.17	−26.00	−21.78		
N28	K1q3	453.8–590.7	95.36	0.750	0.00	0.00	0.00	0.00	0.00	0.00	3.89	0.00	−46.48	−27.67	−22.63	−25.69	
N31	K1q3	538–544	93.63	1.810	0.430	0.300	0.140	0.090	0.050	0.09	2.59	0.86	−42.09	−29.36	−27.37	−27.30	
N3	K1q3	691–696	78.23	2.320	0.870	0.350	0.00	0.060	0.00	0.00	17.89	0.27	−46.43	−30.24	−28.07	−27.30	
N5	K1q3	562–566	94.60	1.850	1.020	1.400	0.00	0.00	0.00	0.00	0.00	0.00	−48.50	−32.60	−31.30	−26.20	
Q198	K1q4	2265.6–2268.8	1.19	1.05	0.45	0.04	0.16	0.03	0.08	0.16	1.46	95.39	−47.44	−37.58	−32.39	−29.98	−4.93
Q199	K1q4	2264.4–2268.4	16.85	3.23	2.14	0.19	0.79	0.15	0.44	0.24	5.58	70.40	−47.78	−37.22	−31.72	−30.00	−4.47
WS1	K1d4	1389.2–1449	89.09	0.93								0.11	−28.1	−28.11	−27.94	−28.83	−8.53
FS7	K1d1	3295–3321.6	82.52	1.17								13.08	−28.12	−25.11	−31.8	−30.87	−10.35
S502	FY	1774–1824	95.22	1.45								0.16	−31.62	−30.94	−29.26	−16.76	
S66	Y	1786–1832.4	94.21	1.51								0.15	−27.88	−24.33	−24.01	−27.34	−12.86
S69	Y	1741.6–1924.8	94.86	1.46								0.17	−31.38	−28.89	−28.27	−25.43	−18.14
G31	H	1201.4–1213.2	93.11	2.79								0.34	−49.91	−32.44	−28.56	−27.13	−21.65
ZS8	K_1yc	3152–3159	88.6	1.06								7.5	−22.9	−24.9	−25.4	−26.9	−16

Table 3. Isotopic characteristics of abiogenic alkane gas in the Songliao Basin.

			$\delta^{13}C$ (‰) PDB					
Gas field	*Well*	*Horizon*	*CH_4*	*C_2H_6*	*C_3H_8*	*C_4H_{10}*	*R/Ra*	*Source*
Xingcheng	Xushen-1-1	K_1yc	–28.9	–32.6	–33.3	–34.1	1.1	Dai et al. (2008)
	Xushen-13	K_{2yc}	–28	–32.2	–33.4	–33.1		
	Xushen-5	K_{2yc}	–25.1	–28.9	–29.6	–31.2		
	Xushen-6	K_1sh	–28.3	–33.2	–34.3	–34.6	1	
	Xushen-6-2	K_1yc	–25.9	–32.4	–33.1	–33.7	0.9	
	Xushen-603	K_1yc	–27	–30.4	–32.3	–34.3	1.2	
Shengping	Shengshen-2	K_1yc	–27.8	–29.1	–30.6	–30.8		
	Shengshen-2-1	K_1yc	–26.8	–29.1	–33.5	–36.5	1.8	Dai et al. (2008)
	Shengshen-2-25	K_1yc	–26.6	–28.8	–32.6	–35.7	1.7	
	Shengshengeng-2	K_1yc	–27.2	–28.1	–32.7	–34.7	1.8	
Changde	Fangshen-1	K_1d	−18.9	−22.8	–25.3	–27.6		
	Fangshen-2	K_1d	−17.4	−22.2	–30.5	–31.4	0.6	Dai et al. (2008)
	Fangshen-801	K_1d	–20.6	–24.8	–27.4	–31.4		
	Fangshen-9	K_1d	−18.9	−22.8	–25.3	–27.6	0.58	Dai et al. (2008)
Wangjiatun	Wang-9-12	FY	–23.9	–23.4	–25	–26.7		
	Wang-13-11	FY	–22.4	–24.8	–27.9	–27.9		
	Wang-24-23	FY	–27.9	–27.7	–28.3	–30.2		
Changling	Changshen-1	K_1yc	–24.2	–26.9	–27.2	–34.3	1.9	Dai et al. (2008)
	Changshen-103	K_1d	–22.1	–28.8	–30.9	–33.2	2.1	
Sanzhao	Zhaoshen-8	K_1yc	–22.9	–24.9	–25.4	–26.9		

Table 4. Gas content and isotope composition of inclusions in volcanic reservoirs in the Songliao Basin.

			Gas content (%)		*Carbon isotope (‰)*	
Well	*Depth (m)*	*Lithology*	*CH_4*	*CO_2*	*C_1*	*CO_2*
Xushen-1	3525.6	Felsic grains in volcanic rocks	72.94	27.06	–27.94	−11.92
Xushen-1	3634.8	Volcanic rocks	53.61	46.39	–26.99	−15.08
Xushen-6	3846.6	Volcanic rocks	17.80	82.20	–25.15	−14.75
Xushen-8	3742.8	Rhyolitic breccia	19.87	80.13	–24.46	−13.00
Shengshen-7	3704.7	Tuff	75.74	24.26	–27.48	−15.82
Shengshen-7	3730.8	Tuff	2.10	97.90	–27.96	−15.75
Shangshen-2	3249.78	Calcite veins in coal	1.78	98.22	–28.47	−10.97
Zhaoshen-3	2886.9	Volcanic rocks	93.64	6.361	–21.42	−16.80
Changshen-1	3574.7	Volcanic rocks	47.63	52.37	–22.85	−12.70
Changshen-103	3724.9	Calcite veins in coal	11.06	88.94	–24.64	−16.45
Changshen-103	3731.8	Calcite veins in coal	79.55	20.45	–24.19	−18.90

sediments (Tao et al., 2012). The homogenization and freezing temperatures for individual inclusions were determined for inclusions in quartz overgrowth material, micro-fissures in clastic quartz grains, and sparry calcite cement in interparticle pores in sandstone (Table 5 and Figure 6).

Table 5. Inclusion data for in volcanic rocks and clastics in the Songliao Basin.

Well	Horizon	Depth (m)	Lithology	Mineral occurrence	Homo-temperature (°C) Range	Homo-temperature (°C) Mean	Salinity (%NaCl) Range	Salinity (%NaCl) Mean
Shengshen-4	Deng-2 member	2941	Gritstone	Early calcite cement	116–165	142.86	1.74–2.41	2.106
Shengshen-4	Deng-2 member	2941	Gritstone	Quartz clast	117–120	118.67	1.74–2.41	2.020
Shengshen-7	Jurassic	3730.8	Calcite vein in grey metamorphic rocks	Calcite filled later in pores and vugs	157–168	163.73	0.88–1.23	1.054
Shengshen-7	Jurassic	3730.8	Calcite vein in grey metamorphic rocks	Barite mineral in calcite vein	130–163	148.20	1.74–2.07	1.905
Shengshen-1	Denglouku	2660.31	Grey white medium sandstone	Quartz clast	97–120	105.89	0.53–1.74	1.190
Shengshen-1	Denglouku	2660.31	Grey white medium sandstone	Quartz overgrowth boundary	103–108	105.55	0.71–0.88	0.838
Shangshen-2	Jurassic	2805.83	Grey white conglomerate-bearing gritstone	Quartz clast	115–127	119.71	1.74–2.57	2.045
Shangshen-2	Jurassic	2805.83	Grey white conglomerate-bearing gritstone	Quartz overgrowth boundary	121–128	124.44	0.53–0.88	0.763
Shangshen-2	Jurassic	2805.83	Grey white conglomerate-bearing gritstone	Calcite cement	119–147	133.00		
Shangshen-2	Jurassic	3249.78	Quartz vein in coal	Late-filling quartz in fractures and vugs	130–139	135.50	3.39–4.34	4.023
Shengshen-201	Deng-2 member	2833.61	Light brown medium to gritstone	Quartz clast	117–124	120.60	11.89–13.2	12.55
Shengshen-201	Deng-2 member	2833.61	Light brown medium to gritstone	Quartz clast	127–134	129.4	1.4–1.74	1.57
Xushen-21	Yingcheng Formation	3659.74	Grey white medium sandstone	Quartz fragment	135–160	151.73	3.39–3.87	3.590
Xushen-1	Lower Cretaceous	4231.82	Grey brown medium and fine sandstones	Fracture-filled calcite	142–150	147.33	3.39–4.18	3.983
Xushen-1	Lower Cretaceous	3525.6	Volcanic pyroclastics	Quartz-1	150–162	156.63	3.39–4.18	3.934
Xushen-1	Lower Cretaceous	3525.6	Volcanic pyroclastics	Quartz-2	125–146	135.20	3.55	3.55
Dashen-1	Lower Cretaceous	3220.32	Green grey andesite	Fracture-filled calcite	130–140	135.25	1.57–1.91	1.683

(continued)

Table 5. Continued

Well	Horizon	Depth (m)	Lithology	Mineral occurrence	Homo-temperature (°C) Range	Homo-temperature (°C) Mean	Salinity (%NaCl) Range	Salinity (%NaCl) Mean
Fangshen-1	Deng-4 member	3024.23	Grey white medium and fine sandstones	Quartz clast	123–126	124.86	11.89–13.82	12.95
Fangshen-1	Deng-4 member	3024.23	Grey white medium and fine sandstones	Quartz overgrowth boundary	121	121.00	0.53	0.530
Fangshen-1	Deng-4 member	3024.23	Grey white medium and fine sandstones	Quartz clast	124–128	126.20	1.05–2.55	1.588
Xushen-6	Lower Cretaceous	3846.62	Volcanic rocks	Quartz	133–169	150.86	1.74–2.74	2.033
Xushen-6	Lower Cretaceous	3846.62	Volcanic rocks	Fracture-filled calcite	170	170.00	3.39	3.390
Wang-902	Deng-3 member	2707.78	Grey white medium and fine sandstones	Quartz clast	108–127	119.17	17.34–17.96	17.608
Wang-902	Deng-3 member	2707.78	Grey white medium and fine sandstones	Quartz overgrowth boundary	119–125	122.67	1.23–1.74	1.485
Dashen-2	Lower Cretaceous	3861.04	Heavy grey medium sandstone	Quartz fragment	143–155	148.80	4.96–6.01	5.440
Dashen-2	Lower Cretaceous	3861.04	Heavy grey medium sandstone	Sparry calcite cement	160–166	163.80	2.57–2.74	2.655
Songshen-3	Jurassic	3290.54	Green grey andesite	Vug-filled calcite	130–140	134.95	1.74–2.74	2.395
Songshen-1	Jurassic	3479.42	Heavy grey gritstone	Quartz clast-1	117–133	128.46	1.4–2.74	1.94
Songshen-1	Jurassic	3479.42	Heavy grey gritstone	Quartz clast-2	103	103		
Songshen-1	Jurassic	3479.42	Heavy grey gritstone	Quartz clast-3	138–141	139.67	1.4–3.23	2.315
Zhaoshen-3	Basement	2886.91–2902.1	Volcanic pyroclastics	Quartz clast	114–126	120.67	1.4–2.41	1.738
Zhaoshen-3	Basement	2886.91–2902.1	Volcanic pyroclastics	Feldspar clast	151–169	164.43	1.91–2.74	2.372
Fangshen-2	Lower Cretaceous	2884.83	Grey medium sandstone	Quartz clast	120–130	124.29	1.74–3.74	2.820
Fangshen-2	Lower Cretaceous	2884.83	Grey medium sandstone	Quartz overgrowth boundary	138–144	140.50	2.24–4.06	2.957
Fangshen-2	Lower Cretaceous	2884.83	Grey medium sandstone	Calcite cement	144	144.00		
Fangshen-2	Lower Cretaceous	2884.83	Grey medium sandstone	Quartz cement	145	145.00		
Tongshen-1	Lower Cretaceous	3074.9–3077	Steel grey fine sandstone	Quartz clast	127–140	135.17	1.74–5.71	3.103

(continued)

Table 5. Continued

Well	Horizon	Depth (m)	Lithology	Mineral occurrence	Homo-temperature (°C)		Salinity (%NaCl)	
					Range	Mean	Range	Mean
Tongshen-1	Lower Cretaceous	3074.9–3077	Steel grey fine sandstone	Quartz clast	135–150	145.17	14.77–15.96	15.29
Tongshen-1	Lower Cretaceous	3074.9–3077	Steel grey fine sandstone	Calcite cement	148–160	154.80	3.23	3.230
Gushen-1	Lower Cretaceous	4489.92	Tuff	Quartz fissure	154–190	172.00	1.23–2.57	1.870
Gushen-1	Lower Cretaceous	4489.92	Tuff	Quartz	147–151	149.17	1.74–1.91	1.797
Pushen-1	Lower Cretaceous	5344.5	Quartz and calcite-bearing volcanics	Fracture-filled calcite	144–160	151.00	2.24–3.23	2.570
Zhaoshen-1	Lower Cretaceous	1748–1756	Grey white fine sandstone	Quartz clast	120–123	121.33	0.88–3.55	1.827
Zhaoshen-1	Lower Cretaceous	1748–1756	Grey white fine sandstone	Quartz clast	97–107	102.00	2.07	2.070
Fangshen-7	Lower Cretaceous	3192–3189	Medium to gritstones	Quartz clast	120–132	126.92	10.48–11.89	11.260
Fangshen-7	Lower Cretaceous	3192–3189	Medium to gritstones	Feldspar overgrowth boundary	140–142	141.00	1.4–1.74	1.570
Fangshen-7	Lower Cretaceous	3192–3189	Medium to gritstones	Quartz overgrowth inside boundary	132	132.00	0.53	0.530
Fangshen-7	Lower Cretaceous	3192–3189	Medium to gritstones	Sparry calcite cement	152	152.00		
Changshen-1-2	Lower Cretaceous	3502.14	Medium and fine sandstones	Quartz clast	120–137	129.40	11.7	11.70
Changshen-1-2	Lower Cretaceous	3502.14	Medium and fine sandstones	Sparry calcite Cement	137–148	142.20	4.65	4.650
Changshen-1-2	Lower Cretaceous	3672	Tuff	Quartz	136–140	138.00	3.23–5.41	4.010
Changshen-1-1	Lower Cretaceous	3728	Sandy conglomerate	Pore and Vug-filled calcite	140–149	145.94	4.96–5.71	5.389
Changshen-1	Lower Cretaceous	3574.7	Tuff	Quartz	136–144	140.70	2.57–3.71	3.197
Laoshen-1	Lower Cretaceous	2574	Medium sandstone	Calcite cement	142–152	147.33	1.23–1.74	1.528
Laoshen-1	Lower Cretaceous	2574	Medium sandstone	Quartz clast	97–101	99.33	2.74–3.39	3.120
Laoshen-1	Lower Cretaceous	2574	Medium sandstone	New quartz	93	93.00	1.74	1.740
Laoshen-1	Lower Cretaceous	3651.8	Calcite vein in igneous rocks	Calcite vein	145–152	149.40	2.07–2.57	2.280
Changshen-103	Lower Cretaceous	3731.8	Calcite vein in volcanic rocks	Giant crystal calcite	161–177	168.84	2.07–2.57	2.396
Changshen-103	Lower Cretaceous	3725.8	Calcite vein in volcanic rocks	Giant crystal calcite	145–157	149.50	2.9–3.71	3.448
Changshen-3	Lower Cretaceous	2669.9	Maroon volcanic rocks	Quartz in pores and fractures	105–110	107.80	0.18–0.71	0.488

Analysis and discussion

Origin of natural gas: Organic or inorganic. The isotopic compositions of organic alkane gases become heavier with increasing carbon numbers of the molecules in some wells, i.e. $\delta^{13}C_1 < \delta^{13}C_2 < \delta^{13}C_3 < \delta^{13}C_4$. In other wells in the Songliao Basin, alkane gases have the exact opposite characteristic, i.e. $\delta^{13}C_1 > \delta^{13}C_2 > \delta^{13}C_3 > \delta^{13}C_4$, and $R/Ra > 0.5$ (Tables 2 and 3, Figure 2), indicating features of abiogenic alkane gas. The analysis of the carbon isotopic compositions of gas from the deep strata in the Songliao Basin shows that the gas is derived from multiple origins (Figure 3). The gas with a high CO_2 content is mainly abiogenic in origin. Generally, the gas in reservoirs near volcanic channels or deep faults has a high content of carbon dioxide and deep mantle source abiogenic characteristics, while gas with a low content of carbon dioxide and an organic origin is generally found in reservoirs far from lava channels or deep faults.

The carbon dioxide content and carbon isotope composition of gas in the Songliao Basin vary greatly (Table 2 and Figure 4). The study of global CO_2 shows that the $\delta^{13}C$ values of organic CO_2 are less than −9‰, the $\delta^{13}C$ values of CO_2 from mantle-derived magma falls between −4 and −8‰, and the $\delta^{13}C$ value of CO_2 generated by the decomposition of carbonate rocks mostly ranges from −3.5 to 3.5‰, due to the inherited nature of the parent material (Poreda et al., 1992). The $\delta^{13}C$ value of the CO_2 from both crustal and mantle magma is within −4 to 10‰, but the $^3He/^4He$ ratio of CO_2 from crustal magma differs from

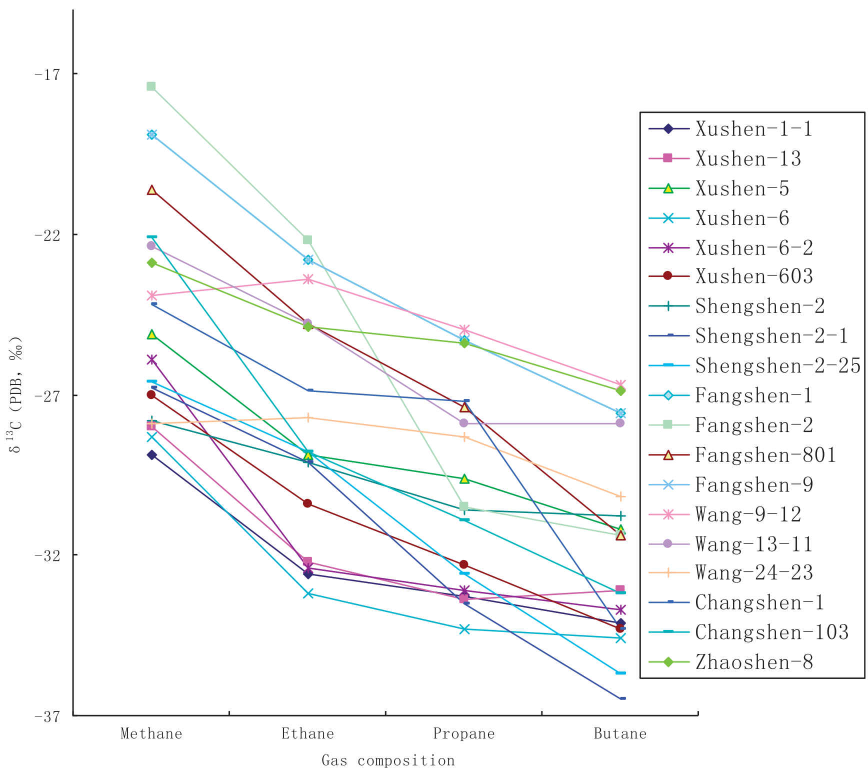

Figure 2. Gas composition versus methane isotopes for some gas wells in the Songliao Basin.

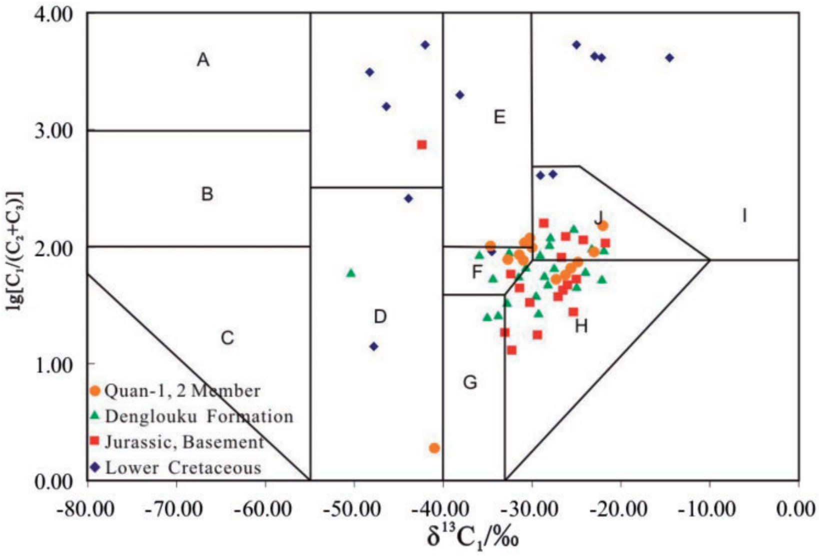

Figure 3. Isotope composition and origin distribution of gas in the Songliao Basin. A. Biogas, B. biogas and sub-biogas, C. sub-biogas, D. crude oil-associated gas, E. oil-associated gas, F. oil-associated and coal-derived gas, G. gas associated with condensate and coal-derived gas, H. coal-derived gas, I. abiogenic gas, and J. abiogenic gas and coal-derived gas.

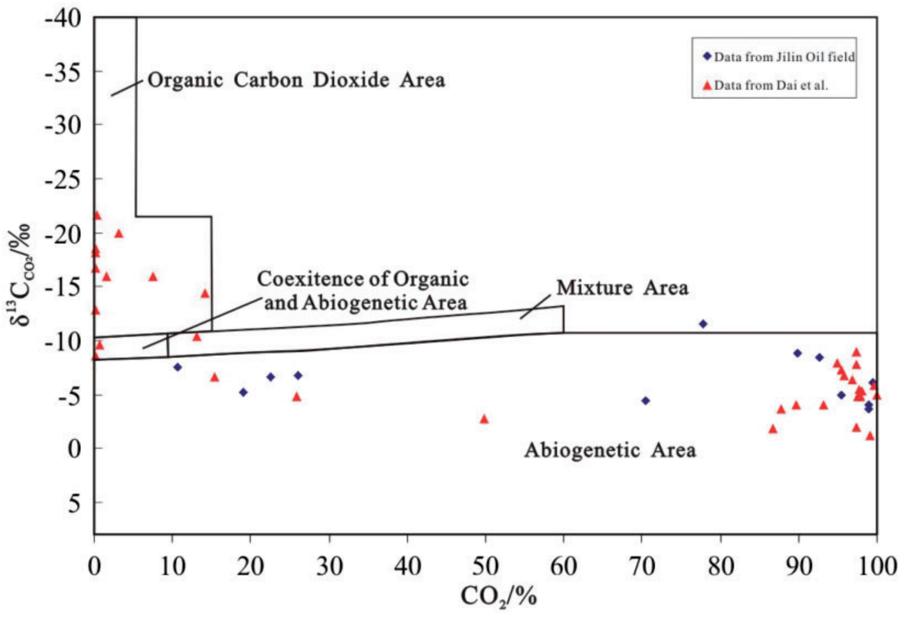

Figure 4. Carbon dioxide contents and carbon isotope compositions of gas in the Songliao Basin.

that of mantle magma. Generally, the CO_2 contents and $\delta^{13}C$ values of a gas reservoir can be used to determine the CO_2 is biogenic or abiogenic. The diagram of carbon dioxide content versus gas carbon isotope values shows that the gas of the Songliao Basin plots in the abiogenic area (Figure 4).

The carbon isotope compositions of alkane gas and CO_2 show the geochemical characteristic differences between the gas in fluid inclusions and in the present gas reservoir. In Table 3, the $\delta^{13}C_{CH4}$ values of inclusions in volcanic rocks range from −17 to −27‰, and the $\delta^{13}C_{CO2}$ values range from −10 to −21‰ in the northern Songliao Basin. In the southern Songliao Basin, the $\delta^{13}C_{CH4}$ values are mainly between −22 and −28‰, and the $\delta^{13}C_{CO2}$ values are between −12 and −18‰. Additionally, the amount of CO_2 in inclusions in the south is less than that in the north. The gas composition of inclusions differs considerably from that in the present reservoirs (in the present gas reservoirs, the amount of CO_2 in the south is much higher than that in the north, reaching percentages as high as 90%, and the carbon isotope values are higher; see Table 2), indicating that the carbon dioxide was more recently injected into the deep gas formations of the Songliao Basin and is mainly of abiogenic origin ($\delta^{13}C_{CO2} > -10‰$, $CO_2 > 60\%$).

The CO_2 content of the present gas reservoirs is 15–98.9%, with many contents greater than 60%, and the CO_2 carbon isotope values are high, between −4 and −8‰ (Table 2), suggesting that the CO_2 in the present gas reservoirs differs from that in inclusions (Table 4). The reservoir CO_2 is abiogenic in origin, while the inclusion of CO_2 is organic in origin. The CH_4 content of the present gas reservoirs is 0.41–77.85%, and the carbon isotope values range from −16.8 to −51.1‰, suggesting that the CH_4 in the present reservoirs is of mixed organic and abiogenic origin but is associated with mantle-released He to varying degrees.

Based on these observations, the gas in the volcanic reservoir in the Songliao Basin displays the following characteristics: first, the gas in many wells has characteristics of $\delta^{13}C_{CH4} > -30‰$ and $\delta^{13}C_1 > \delta^{13}C_2 > \delta^{13}C_3 > \delta^{13}C_4$; second, the gas in most wells has CO_2 characteristics of $\delta^{13}C_{CO2} > -10‰$ and $CO_2 > 60\%$; third, all R/Ra ratios of inclusions and present gas samples are greater than 0.5; and fourth, the distribution and enrichment of some gas reservoirs are controlled by deep faults and volcanic craters. The He and Ar isotopic data from inclusions (Tao et al., 2012) show that gas channels connect the mantle to the deep strata in the Songliao Basin. Based on the present gas reservoir isotopic values, the origin of the gas features multiple sources dominated by abiogenic processes (Dai, 1992, 2009; Tao et al., 2012; Wakita and Saio, 1993; Zhang et al., 2007; Zhu et al., 2005).

Source of the natural gas: Mantle or crust. The deep volcanic formations in the Songliao Basin developed during the rifting period of East China, when channels allowed gas generated by deep hydrothermal fluid activity to migrate to the reservoirs and flourishing terrestrial plants provided an organic gas source. The resulting gas in the volcanic reservoirs in the Songliao Basin is therefore derived from multiple sources and origins.

Using noble gas composition, it is possible to determine whether the volcanic gas was sourced from the crust or the mantle. Rare gases, such as He and Ar, have two sources, the crust and the mantle, which have quite different ratios of $^3He/^4He$ and $^{40}Ar/^{36}Ar$. The $^3He/^4He$ ratio of the gas in the Songliao deep strata falls in between 0.286×10^{-6} and 7.33×10^{-6} (Tao et al., 2012), with an average of 2.48×10^{-6}. Therefore, a He–Ar isotope distribution diagram is used to assess the gas origins by dividing crust or mantle gas types. Among the 37 samples of volcanic rock inclusions from the Songliao Basin, 32 have $^3He/^4He$ ratios on the order of 10^{-6}, plotting in the crust–mantle mixture area of the He–Ar isotope distribution diagram

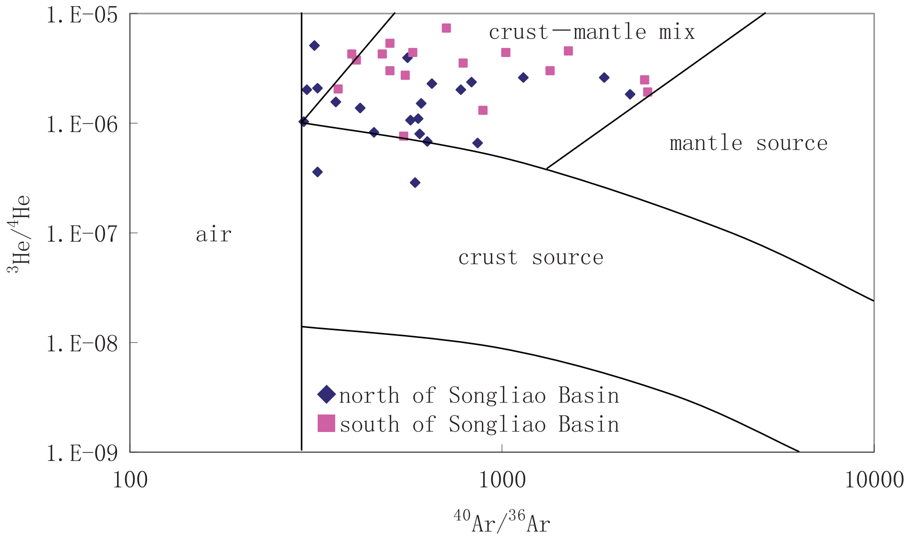

Figure 5. Helium–Argon isotope distribution diagram for the volcanic rocks inclusions from the Songliao Basin.

(Figure 5), indicating the existence of mantle-released He in the gas and minor gas from a crustal source. The $^{40}Ar/^{36}Ar$ ratio ranges from 293 to 2485, with an average of 796.7, which together with the ratio of $^{3}He/^{4}He$, also indicates a crust–mantle mixture characteristic. Both ratios also indicate that the tectonic activity was intense in the Songliao Basin and that deep faults and channels acted as conduits for magma derived from the mantle. Furthermore, the He R/Ra values (the ratio of the $^{3}He/^{4}He$ ratio of the sample to the $^{3}He/^{4}He$ ratio of the air) of the inclusions in volcanic rocks and nearby clastic rocks in the Songliao Basin are high, with most being greater than 1.0, further supporting the mantle source characteristics.

The inclusions in the southern part of the Songliao Basin have much higher R/Ra values than those in the northern part and therefore contain more mantle-released He in the natural gas. The R/Ra values of inclusions in the Changling rift volcanics rise gradually from the southeast to the northwest (Tao et al., 2012), indicating an increase in mantle-released He. Exploration practices have also shown that many high CO_2 content gas wells have been drilled in the northwest of Changling, such as the wells Changshen-3, -4, and -6, which have CO_2 contents of over 90%. It can be seen that high value area of mantle-released He is consistent with the area of high CO_2-content gas reservoirs.

As discussed above, the area with high R/Ra values is consistent with faults and volcanic craters with high contents of mantle-released He in the Songliao Basin. Thus, the area with high R/Ra values is an abiogenic gas area. It can be seen from the R/Ra distribution map that Well Fangshen-2 and Fangshen-7, which have R/Ra values of >1.5, are located in the vicinity of faults or volcanic craters (Tao et al., 2012).

The above analysis indicates that the distribution of isotopic compositions of alkane gases in the volcanic reservoirs is complex (Table 2), with both positive carbon isotope series ($\delta^{13}C_1 < \delta^{13}C_2 < \delta^{13}C_3 < \delta^{13}C_4$) and negative carbon isotope series ($\delta^{13}C_1 > \delta^{13}C_2 > \delta^{13}C_3 > \delta^{13}C_4$). Therefore, the volcanic gas in the Songliao Basin consists of both organic gas and inorganic gas. Additionally, the carbon isotope compositions vary widely.

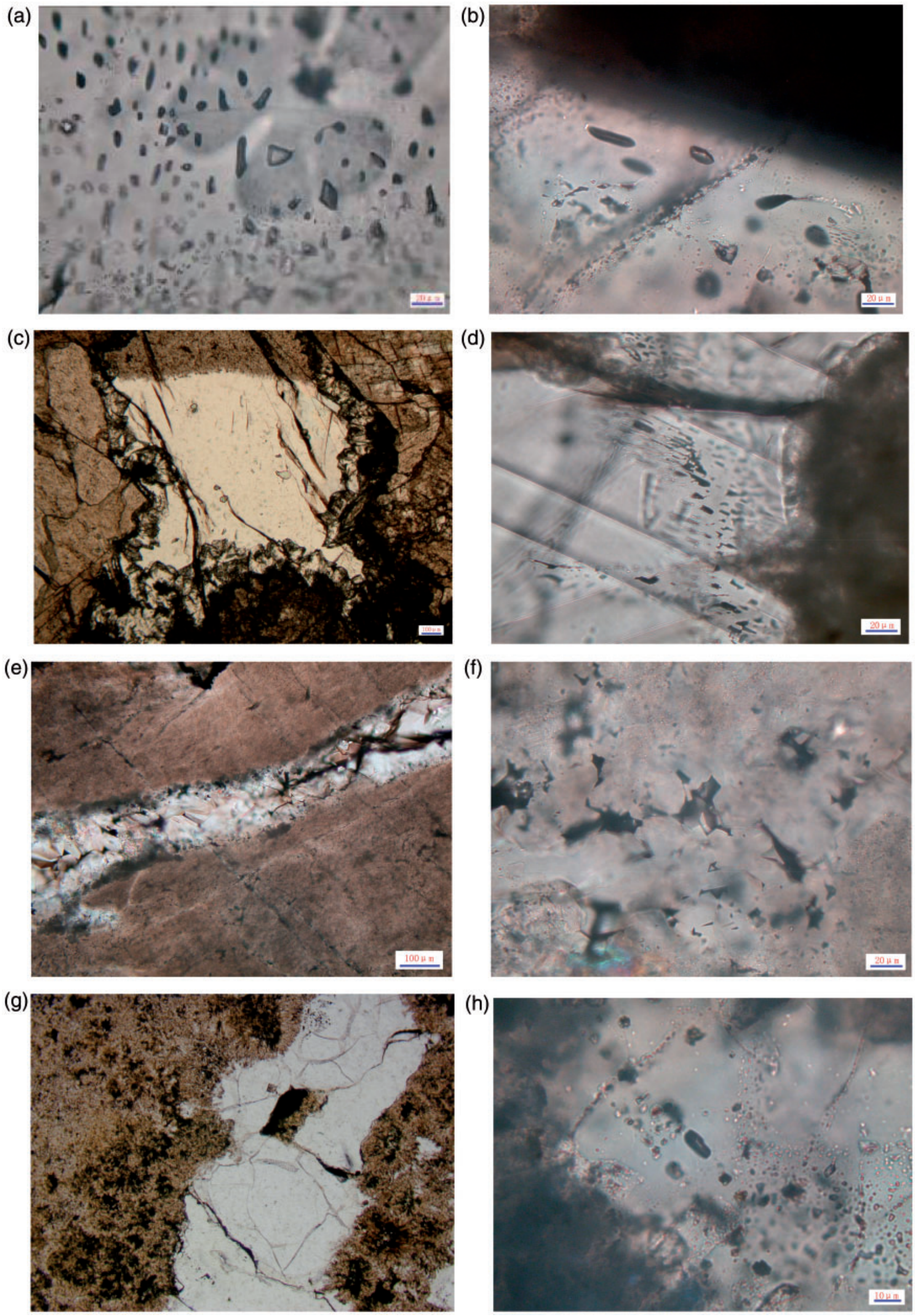

Figure 6. Gaseous hydrocarbon inclusions in volcanic and clastic rocks in the Songliao Basin. (a) Well Changshen-103, 3731.8 m depth, grey gaseous inclusions in belt shape in giant crystal calcite in carbonate veins in a tuffaceous breccia. (b) Well Changshen-1-2, 3612 m depth, gaseous inclusions in belt shape and

For example, the $\delta^{13}C_2$ values are −20.73 to 37.58‰, with the majority below −28‰. Alkane gases that have positive isotope series or mostly positive isotope series are oil-associated gas when $\delta^{13}C_2 < -28$‰ and coal-derived gas when $\delta^{13}C_2 > -28.5$‰ (Dai et al., 2008). Therefore, the organic gases in the volcanic rocks of the Songliao Basin are mainly coal-derived gas. The carbon isotope values of CO_2 also vary widely, with $\delta^{13}C_{CO_2}$ ranges from −1.82 to −21.65‰. Usually, the $\delta^{13}C_{CO_2}$ values are lower than −10‰, indicating that the CO_2 is both organic and inorganic in origin. The following analysis shows that the main charge and accumulation periods of the organic gas are different from those of the inorganic gas. All the fluid inclusion results show that the formation of the organic gas reservoirs (approximately during the late Cretaceous) occurred earlier than that of the inorganic gas (mainly in the late Paleogene).

Natural gas charging period and components. The systematic temperature tests of the volcanic rock inclusions show that the fluid inclusions have homogenization temperatures that range from 93 to 190°C and salinities that range from 0.18–17.96% NaCl, indicating that the reservoir rocks and fluid evolution vary distinctly among different wells. Therefore, the gas charging period can be identified by the homogenization temperatures and thermal evolution history. For example, the inclusions in quartz clasts and sparry calcite cement from Well Changshen-1-2 have homogenization temperatures of 120–137 and 137–148°C, respectively, and salinities of 11.7 and 4.65% NaCl, respectively, indicating that the fluids in the inclusions were captured in two different periods. According to the thermal and burial history of this area (Nicole et al., 2008), the two captured periods are the late Cretaceous (K_2) at 75 Ma and Eocene (E_2) at 45 Ma, suggesting a two-stage charging history involving an early period of hydrocarbon gas charge and a late period of carbon dioxide charge. The Yingcheng Formation of Well Changshen-103 has brine inclusions associated with gaseous inclusions that have an average capture temperature of 149.5°C and brine inclusions associated with gaseous CO_2 inclusions with an average capture temperature of 168.8°C. Therefore, it is believed that the well area of Changshen-103 also has a two-stage charge history involving a K_2 stage of hydrocarbon charge and E_2 stage of carbon dioxide charge.

The above analyses indicate that the volcanic natural gas in the Songliao Basin is a mixture of organic coal-derived gas and inorganic mantle-released gas. Different types of gas have obviously different accumulation control factors: the formation and distribution of organic

Figure 6. Continued
their associated colourless and grey saline inclusions in quartz crystals in a rhyolite and magma-fragmented tuff. (c) Well Shengshen-7, 3730.8 m depth, Jurassic calcite-bearing volcanic rocks with two stages of calcite, an early dark grey stage with some alteration and a late fresher and transparent stage that filled in early intergranular pores and vugs. (d) Well Shengshen-7, 3730.8 m depth, dark brown aqueous hydrocarbon inclusions in strip distribution in calcite crystals in Jurassic volcanic rocks with calcite veins. (e) Well Shangshen-2, the Jurassic strata at 3249.18 m depth, medium-late quartz veinlets (bright strip) in quartz veins with clasts of thermo-fluid origin. (f) Well Shangshen-2, the Jurassic strata at 3249.18 m depth, grey gaseous hydrocarbon inclusions in clusters in late-stage quartz veinlets in quartz veins. (g) Well Xushen-6, the lower Cretaceous strata at 3846.62 m depth, amygdaloidal trachyte with phanerocrystalline quartz crystals (most < 0.2 mm) between spherulite structured rocks, hyalopilitic structure. (h) Well Xushen-6, the lower Cretaceous strata at 3846.62 m depth, grey gaseous hydrocarbon inclusions in strip distribution in amygdaloidal trachyte.

gas is controlled by coal measure source rocks in the hydrocarbon generation sag, while the formation and distribution of inorganic gas is controlled by deep fault, volcanic conduit, and volcanic reservoirs. Consequently, the selection of exploration directions and targets for the volcanic gas varies significantly: the coal measure source rocks in the hydrocarbon generation sag and the peripheral volcanics are favourable for the exploration of organic gas, while the vicinity of volcanic conduits and volcanic reservoirs is favourable for inorganic gas.

Conclusions

The Songliao Basin developed widespread volcanic hydrocarbon reservoirs during its fault depression period. The rocks are mainly intermediate-basic rocks in the northern part, intermediate-acidic rocks in the Xujiaweizi area in the southern part, and acidic rocks in the Jinglin block. The gas in the volcanic reservoirs, which varies widely in composition, is mostly alkane gas, but in some wells, carbon dioxide dominates. Generally, the gas in volcanic reservoirs near deep faults and volcanic rock fracture zones has the mantle-derived characteristic of a high carbon dioxide content, while the gas from shallow source rocks in reservoirs far from deep faults and volcanic fracture zones has a low carbon dioxide content.

The gas in volcanic reservoirs of the Songliao Basin was sourced from multiple origins. The gas with high CO_2 contents is mostly abiogenic gas. The carbon isotope sequence of abiogenic alkanes decreases, i.e. $\delta^{13}C_1 > \delta^{13}C_2 > \delta^{13}C_3 > \delta^{13}C_4$, which is the opposite of that of gas with an organic origin.

The rare gases of the volcanic rocks in the Songliao Basin are from two sources, the shallow crust and the mantle, and the value of $^3He/^4He$ in the fluid inclusions in the volcanic reservoirs ranges from 0.286×10^{-6} to 7.33×10^{-6}, with an average of 2.48×10^{-6}. Additionally, $R/Ra = 0.26$–5.24, and in most cases $R/Ra > 1$, indicating a mixture of He from the crust and the mantle. The carbon isotope values of gas in the volcanic inclusions are as follows: $\delta^{13}C_1$: −17.1 to −28.7‰, $\delta^{13}C_2$: −23.4 to −32.4‰ (approximately −25‰ in most cases), and $\delta^{13}C_{CO_2}$: −10.97 to −21.73‰. These values are quite different from the isotopic composition of the gas in the present gas reservoirs. This reflects the complexity of gas charging from different sources during different periods. During the geologic history of the basin and the main accumulation periods, some abiogenic alkane was charged into the reservoirs. The early charged CO_2 is mainly of organic origin, while abiogenic CO_2 was charged during the main accumulation period. In summary, the gas in the volcanic reservoirs in the Songliao Basin is a mixture of abiogenic gas and organic gas.

The abiogenic alkane, CO_2, He, and high CO_2 content data indicate abiogenic gas is present in the reservoirs of the Songliao Basin. According to the relationship between the distribution and occurrence of volcanic rocks and fault activity, the abiogenic gas reservoirs are located near fault zones, while organic and mixed gas reservoirs are located far from fault zones.

Acknowledgements

The authors would like to thank postdoctoral cooperation supervisor Dai Jinxing, academician, for the guidance and help! Additionally, thanks are extended to Jilin and Daqing Oilfield Research Institute of Petroleum Exploration and Development for sample collection during the research.

Declaration of conflicting interests

The author(s) declared no potential conflicts of interest with respect to the research, authorship, and/or publication of this article.

Funding

The author(s) disclosed receipt of the following financial support for the research, authorship, and/or publication of this article: This study was supported by the PetroChina Major Scientific and Technical Project (No. 2014B-0608) and the National Science and Technology Major Project of China (No. 2011ZX5001-001).

References

Dai J (1992) Identification and distinction of various alkane gases. *Science in China (Series B)* 35(10): 1246–1257.
Dai J, Ni Y and Huang S (2014) The significance of the coal-derived study for development of natural gas industry development in China. *Natural Gas Geoscience* 25(1): 1–22.
Dai J, Qin S, Tao S, et al. (2005) Development trend of natural gas industry and important progress of theory of gas geoscience in China. *Natural Gas Geoscience* 16(2): 127–141.
Dai J, Zou C, Zhang S, et al. (2008) Discrimination of abiogenic and biogenic alkane gases. *Science in China (Series D)* 5(12): 1737–1749.
Feng Z (2008) Volcanic rocks as prolific gas reservoir: A case study from the Qingshen gas field in the Songliao Basin, NE China. *Marine and Petroleum Geology* 25: 416–432.
Gao R and Cai X (1997) *The Formation Conditions and Distribution Rule of Oil and Gas Field of Songliao Basin*. Beijing: Petroleum Industry Press, pp. 104–137.
Guo Z and Wang X (1994) Study on biogenic gas in Songliao Basin. *Science in China (B)* 24(3): 303–309.
Huang F (1996) Study on the chemical composition, genetic types and distribution characteristics of natural gas in northern Songliao Basin. *Gas Industry* 16(4): 3–9.
Huang H (2000) Study on gas isotope reverse in deep Xujiaweizi fault depression in northern Songliao Basin. *Earth Science – Journal of China University of Geosciences* 25(6): 617–622.
Li X, Peng S and Shao M (2009) Gas origin analysis and source correlation in deep Songliao Basin-taking Yingcheng formation gas reservoir in Block Changshen1 of Changling fault depression as an example. *Gas Industry* 29(11): 5–8.
Nicole AS, Samuel N and Karsten MH (2008) Plume–ridge interaction revisited: Evidence for melt mixing from He, Ne and Ar isotope and abundance systematics. *Earth and Planetary Science Letters* 268(3–4): 424–432.
Poreda RJ, Craig H, Arnorsson S, et al. (1992) Helium isotopes in Icelandic geothermal systems: I. ^{3}He, gas chemistry, and ^{13}C relations. *Geochimica et Cosmachimica Acta* 56(12): 4221–4228.
Ren Y, Zhu D, Wan C, et al. (2004) Geologic features and gas exploration direction in deep northern Songliao Basin. *China Petroleum Exploration* 4: 12–18.
Tao S, Dai J, Zhou C, et al. (2012) The trace of the reason of genesis, formation and mineral resources of natural gas and rare gas isotope existing in volcanic inclusion of Songliao Basin. *Acta Petrologica Sinica* 28(3): 927–938.
Wakita H and Saio Y (1993) $^{3}He/^{4}He$ ratios in CH_4 rich natural gases suggest magmatic origin. *Nature* 305: 792–795.
Wang X, Tuo J and Zhou S (2006) Discussion on natural gas formation mechanism and the related earth science questions. *Natural Gas Geoscience* 17(1): 7–13.
Yang F, Wang Y and Yang B (2002) Accumulation history research of natural gas system in northern Songliao Basin. *Journal of Chengdu University of Technology* 29(6): 621–626.

Zhang S, Liang D, Zhu G, et al. (2007) Fundamental geological elements for the occurrence of Chinese marine oil and gas accumulations. *Chinese Science Bulletin* 52(A01): 28–43.

Zhu G, Zhang S, Liang Y, et al. (2005) Isotopic evidence of TSR origin for natural gas bearing high H2S contents within the Feixianguan formation of the Northeastern Sichuan Basin, southwestern China. *Science in China* 48(11): 1960–1971.